coatings

MDPI

Article

Tribocatalytic Reaction Enabled by TiO_2 Nanoparticle for MoDTC-Derived Tribofilm Formation at ta-C/Steel Contact

Daiki Matsukawa [1], Jae-Hyeok Park [2], Woo-Young Lee [3], Takayuki Tokoroyama [1], Jae-Il Kim [1,4,*], Ryoichi Ichino [2,5] and Noritsugu Umehara [1]

[1] Department of Micro-Nano Mechanical Science and Engineering, Graduate School of Engineering, Nagoya University, Furo-cho, Chikusa-ku, Nagoya 464-8603, Japan
[2] Institute of Materials Innovation, Institutes of Innovation for Future Society, Nagoya University, Nagoya 464-8601, Japan
[3] Intelligent Optical Module Research Center, Korea Photonics Technology Institute (KOPTI), Cheomdan Venture-ro 108-gil 9, Buk-gu, Gwangju 61007, Republic of Korea
[4] Extreme Materials Institute, Korea Institute of Materials Science, Changwon 51508, Republic of Korea
[5] Department of Chemical Systems Engineering, Graduate School of Engineering, Nagoya University, Nagoya 464-8603, Japan
* Correspondence: xiontioc@gmail.com; Tel.: +81-52-789-2788

Abstract: Tribochemically produced triboproducts are becoming increasingly important in tribosystems and serve to improve system performance by preventing friction or wear. Diamond-like carbon (DLC) is chemically stable, which features a trade-off with tribological pros and cons. Chemically stable DLC is thermally stable and suppresses surface damage in a high-temperature operating environment; however, it causes a detrimental effect that hinders the formation of a competent tribofilm. In this study, we dispersed highly reactive TiO_2 nanoparticles (TDONPs) in molybdenum dithiocarbamate (MoDTC)-containing lubricant for adhering triboproducts on the DLC surface. In addition, TDONPs contributed to the decomposition of triboproducts by promoting the decomposition of MoDTC through its catalytic role. Rutile TDONPs were more helpful in reducing friction than anatase TDONPs and improved the friction performance by up to ~100%.

Keywords: tribocatalyst; MoDTC; TiO_2 nanoparticles; DLC; tribofilm; low friction

check for updates

Citation: Matsukawa, D.; Park, J.-H.; Lee, W.-Y.; Tokoroyama, T.; Kim, J.-I.; Ichino, R.; Umehara, N. Tribocatalytic Reaction Enabled by TiO_2 Nanoparticle for MoDTC-Derived Tribofilm Formation at ta-C/Steel Contact. *Coatings* **2024**, *14*, 773. https://doi.org/10.3390/coatings14060773

Academic Editor: Huirong Le

Received: 30 May 2024
Revised: 14 June 2024
Accepted: 17 June 2024
Published: 19 June 2024

Copyright: © 2024 by the authors. Licensee MDPI, Basel, Switzerland. This article is an open access article distributed under the terms and conditions of the Creative Commons Attribution (CC BY) license (https://creativecommons.org/licenses/by/4.0/).

1. Introduction

The importance of tribochemically generated tribofilms has been emerging in tribological systems [1]. Numerous tribofilms are formed based on thermodynamic factors for the equilibrium state of friction by-products, which provide additional lubrication properties and prevent surface damage, making it an essential factor in determining the efficiency of tribosystems. To this end, oil-soluble additives such as molybdenum dithiocarbamate (MoDTC) and zinc dialkyl dithiophosphates (ZnDTPs), which form a low-shearing and wear-protecting tribofilm, are mainly used in the transportation machinery. Lubricant additives have the advantage of forming affirmative friction by-products during the friction process. Among such additives, MoDTC has long been of interest as an efficient friction modifier because it forms a colloidal MoS_2-containing tribofilm and also serves as an extreme pressure additive [2]. The low-shear MoS_2-based tribofilm is formed by the decomposition and chemical compatibility of MoDTC and exhibits excellent properties in metal-to-metal tribopairs capable of Mo-metal metallic bonding.

In addition, several studies are being actively conducted on the surface treatment of driven engine components for long-term durability. In recent years, awareness of environmental issues has risen, and the trend of miniaturization of engine parts and low viscosity of lubricants has accelerated, expanding the regime of mixed lubrication and boundary lubrication rather than fluid lubrication in various tribosystems [3,4]. Therefore, a technology to prevent wear due to solid contact in boundary lubrication is required, and

it is also required to improve the wear resistance in terms of the material of the engine parts. Today, according to such industrial requirements, tetrahedral amorphous carbon (ta-C) [5,6], one of diamond-like carbon (DLC) with high hardness, chemical stability, and wear resistance, has been pointed out as a suitable hard coating. On the other hand, the superior chemical stability of ta-C acts as a double-edged sword for certain tribosystems. Its chemical stability avoids surface damage in extreme operating environments (e.g., acid-base and high-temperature), but at the same time makes it difficult to react and form triboproducts. As a way to solve this problem, metal-doped DLCs (Me-DLCs) have been studied to increase the reactivity with additives [7–9]. There is a trade-off relationship between the improved lubricity due to the formation of additive-derived tribofilm at the cost of reduced hardness and worse wear resistance; therefore, we need to find a way to solve the technical limitations of these conflicting friction and wear characteristics.

A tribocatalyst is a catalyst that mechanochemically promotes and induces the reaction of materials [10–12]. Nanoparticles (NPs) are a hotspot material as a tribocatalyst because of their large surface area, and their use has been explored early in the field of using existing catalytic reactions such as energy, environment, and battery fields. Nevertheless, this is a rare attempt in the field of friction reduction and is expected to be used as a next-generation additive for lubricants. Unfortunately, their poor dispersibility is a challenge that needs to be addressed at the present stage.

TiC coating [13,14], or Ti-doped DLC [15,16], has excellent triboreaction characteristics and forms a well-developed tribofilm; however, it has the problem of deteriorating the hardness of the DLC and rapidly increasing wear. On the other hand, adding NPs composed of Ti to oil is expected to improve the friction characteristics by forming a tribofilm without deteriorating the ta-C. According to Pauling's valence bonding theory [17], titanium has the fewest d-orbitals among 3*d*, 4*d*, and 5*d*-transition metals. Thus, it is an element with high tribological utilization due to its high reactivity and adhesiveness with other elements. Therefore, highly reactive titanium has high potential as a tribocatalyst [18], and titanium dioxide exists in three major polymorphs: rutile, anatase, and brookite. TiO_2 combines the features of opto-electronic and photo-catalytic characteristics, as well as exhibiting high chemical stability and being non-toxic and affordable. Of these, the rutile phase has a high dielectric constant, which makes it useful for triboelectric applications [19].

In this paper, anatase-phase and rutile-phase titanium dioxide NPs (a-TDONPs and r-TDONPs, respectively) were incorporated into poly alpha-olefin (PAO4) with 700 ppm of MoDTC. Here, we tried to improve the lubricity in the tribopair of ta-C/steel by utilizing the characteristics of valence bonding of Ti and the catalytic characteristics of TiO_2. In addition, the proper amount of TDONPs to be added to improve the friction performance was identified. On the other hand, we did not deal with their long-term precipitation and dispersion, and only short-term dispersion confirmed the sufficient potential of TDONPs as tribological catalysts for future additives.

2. Materials and Methods

The ta-C deposition process is as follows, and a hybrid coating system with an anode-layer ion source (ALIS), unbalanced magnetron sputter (UBMS), and filtered cathodic vacuum arc (FCVA) was used as shown in Figure 1.

A 22.5 mm diameter and 4 mm thick SUJ2 steel disk was used as a substrate for ta-C coating. The substrates were first ultrasonically cleaned with benzene and acetone to remove oil. Secondly, Ar^+ plasma etching was performed using ALIS to remove impurities. Ar gas was discharged at a flow rate of 16 sccm using ALIS, and Ar^+ ions were accelerated at a discharge voltage of 1.8 kV to sputter the substrate for 20 min. In addition, to improve adhesion to ta-C, a 200 nm thick Ti intermediate layer was deposited on the substrate using UBMS. The discharge power of UBMS was 600 W and 25 sccm of Ar for 40 min.

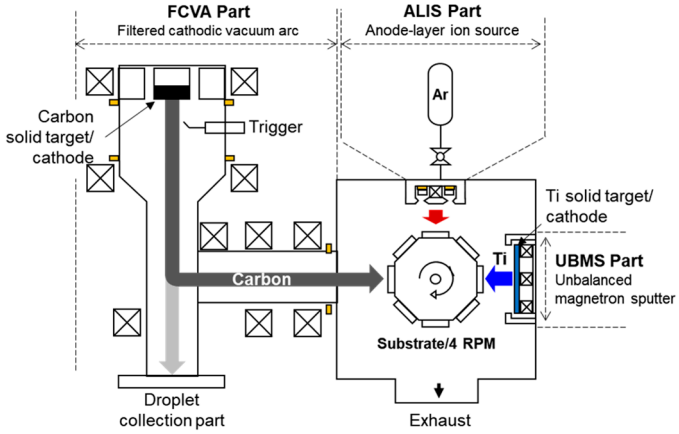

Figure 1. Schematic of hybrid coating system equipped with an anode-layer ion source, filtered cathodic vacuum arc source, and unbalanced magnetron sputter source.

Finally, ta-C was coated with FCVA, which was used in our earlier work [20], to a thickness of approximately 300 nm. The carbon target was discharged with an arc current of 50 A, and carbon ions were accelerated with a substrate bias of −100 V.

a-TDONPs and r-TDONPs (EM Japan Co., LTD., Tokyo, Japan; purity = >3 N; φ = 30 nm) were prepared to confirm their friction properties at similar sizes and purity. Since anatase (H = 12.5 GPa) is chemically more unstable and has a lower hardness than rutile (H = 15.5 GPa), two types of TDONPs were used to compare the difference as tribocatalysts. Anatase is used in the photocatalyst field, and rutile is used as an excellent triboelectric material, so its usefulness in tribocatalysis was evaluated. On the other hand, inorganic TiO_2 has poor surface compatibility with oil, so its dispersing performance is extremely poor. In order to disperse even during the tribotest, we proceeded with the following surface treatment. A technique to improve dispersibility has been reported to react with oleic acid (OA), an organic alteration agent, in n-hexane as oil-based suspensions [21]. Through this, inorganic nanoparticles chemically absorb alkyl canes, increasing the oil affinity of inorganic nanoparticles. First, TDONPs, OA, and n-hexane were ultrasonically mixed at a ratio of 1 g:1 g:100 mL, respectively. After that, the mixed solution was stirred with a magnetic stirrer (AS ONE CHPS-170DF, Osaka, Japan) to evenly treat the surface. For sufficient reaction, the temperature of the solution was set to 60 °C, and the reaction was elicited by stirring for 5 h. After the reaction was complete, the TDONPs were collected on a PTFE membrane filter (Merck Omnipore, Bellerica, MA, USA, pore size: 0.2 μm) by vacuum filtration and washed with isopropyl alcohol and de-ionized water to remove unbound OA and n-hexane. Finally, the OA-modified TDONPs were heated in a furnace at 100 °C for 1 day to evaporate residual moisture and contaminants.

Figure 2a,b show PAO4 lubricants mixed with 2 wt.% of a-TDONPs and OA-modified a-TDONPs after a 2 h friction test. In the case of a-TDONPs without OA treatment, they were moved out of the contact surface by centrifugal force. On the other hand, OA-treated a-TDONPs showed a dispersed appearance even after a 2 h tribological test. However, it was confirmed that it precipitated after a week of mixing. We selected an additive amount of OA-TDONPs up to 2.5 wt.% because the dispersion limit was observed at addition amounts of 2.5 wt.% as shown in Figure 2c. The dispersion improvement occurred over a narrow concentration range, and 2.5 wt.% was too catastrophic for the transition, which was believed to be due to aggregation due to the high free surface energy and reduced electrostatic repulsion that often occur in NPs. OA-modified a-TDONPs were added in an amount of 0–2.5 wt.% to PAO4 with 700 ppm of MoDTC added, and the added mixture was treated in an ultrasonic bath for 2 h to disperse. Hereinafter, 'TDONPs' refer to 'OA-modified TDONPs'.

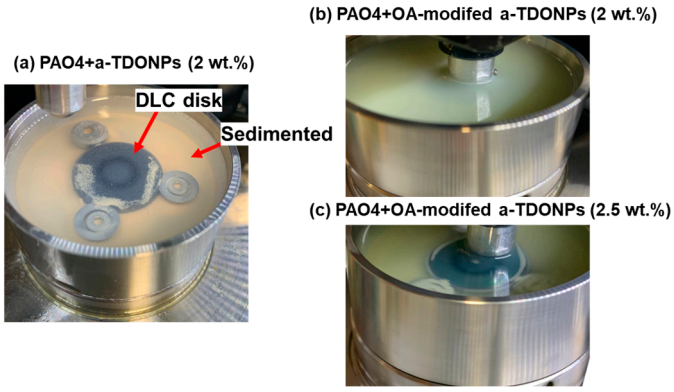

Figure 2. Images after tribotest of lubricant composed of PAO4 base oil with 2 wt.% of (**a**) TDONPs and (**b**) OA-modified TDONPs and (**c**) 2.5 wt.% of OA-modified TDONPs.

The friction performance of TDONPs was evaluated using a ball-on-disk-type tribometer and tribotests were repeated at least 3 times to assure reliability. A ta-C-coated disk and a SUJ2 ball (diameter 8 mm) were utilized as a DLC/steel tribopair. PAO4 mixed with 700 ppm MoDTC and 0–2.5 wt.% TDONPs were heated in an oil bath and functioned as a lubricant. A load of ~10 N was applied using a weight of 1 kg, and the ta-C coated disk rotated at a sliding speed of 34 mm/s for 3 h, corresponding to ~250 m of sliding distance. The maximum contact pressure was ~1.3 GPa, and the coefficient of friction (CoF) was collected in an initial boundary lubrication regime with a Lambda ratio less than 1.

A confocal laser scanning microscope (Olympus OLS5100, Tokyo, Japan) was used to observe the surfaces of the disks and balls after tribotests. In addition, the elemental distribution of the tribofilm was characterized using a scanning electron microscope (SEM; JEOL JCM-5700NU, Tokyo, Japan) equipped with an energy-dispersive X-ray spectroscope (EDS; JEOL EX-54175NU, Tokyo, Japan) at an acceleration voltage of 10 keV. A Raman spectrometer with a laser wavelength of 532 nm (RENISHAW inVia Reflex, Gloucestershire, UK) was used to identify the chemical structure of tribofilm at 1800 lines/mm grating. The chemical composition and bonding ratio of the worn surface were obtained using X-ray photoelectron spectroscopy (XPS; ULVAC PHI Quantera III, Chigasaki, Kanagawa, Japan; X-ray spot size: 50 μm, Al-Kα radiation). The surface was cleaned by pre-sputtering with Ar^+ ions for 12 s before acquiring XPS spectra.

3. Results

3.1. Friction Performance of TiO_2 Nanoparticles with MoDTC Addition

First, 0.0, 1.0, 1.5, 2.0, and 2.5 wt.% of a-TDONPs and r-TDONPs were mixed with lubricating oil in which 700 ppm of MoDTC was added to PAO4 (Figure 3). The friction test was conducted at a temperature of 80 °C, which is similar to the environment of a vehicle engine and where MoDTC can be activated [22]. At this time, the initial Lambda ratio was very low, ~0.05, meaning that friction was almost dominated by solid lubrication. The friction performance of the ta-C/steel tribopair was evaluated at a load of 10 N and a speed of 34 mm/s. As a result, the friction tended to decrease as the addition of a-TDONPs and r-TDONPs increased. The oil without a-TDONPs showed a friction of 0.074, and the oil with 2 wt.% of a-TDONPs and r-TDONPs showed a friction improvement effect of approximately 57% and 100% at 0.047 and 0.037 of friction coefficient, respectively (Figure 4). However, with an addition amount of 2.5 wt.%, the friction increased to 0.063 and fluctuated unstably. It is known that the chemical reaction of MoDTC deteriorates the wear of DLC [9]; therefore, the wear of ta-C was measured, as shown in Figure 4b. As a result, a similar wear rate was observed even when the amount of a-TDONPs was increased to 2 wt.% compared to the case where TDONPs were not added. On the other hand, in the case of r-TDONPs, the wear rate slightly decreased as the addition amount increased up to 2 wt.%. However, as the concentration exceeded 2 wt.%, the wear increased in both the anatase and the rutile. As shown in Figure 2, at the amount of 2.5 wt.% TDONPs

in PAO4, the TDONPs no longer kept their dispersibility and precipitated on the surface and outside of ta-C, which is believed to be the cause of the increase in friction. In addition, a noticeable increase in wear was observed in rutile, which has relatively higher hardness compared to anatase, and it is believed that this caused three-body wear in ta-C, causing a rapid increase in wear. Similar to Figure 2, even extrapolated from friction and wear performance, a maximum of 2.5 wt.% is considered the dispersion limit for TDONPs.

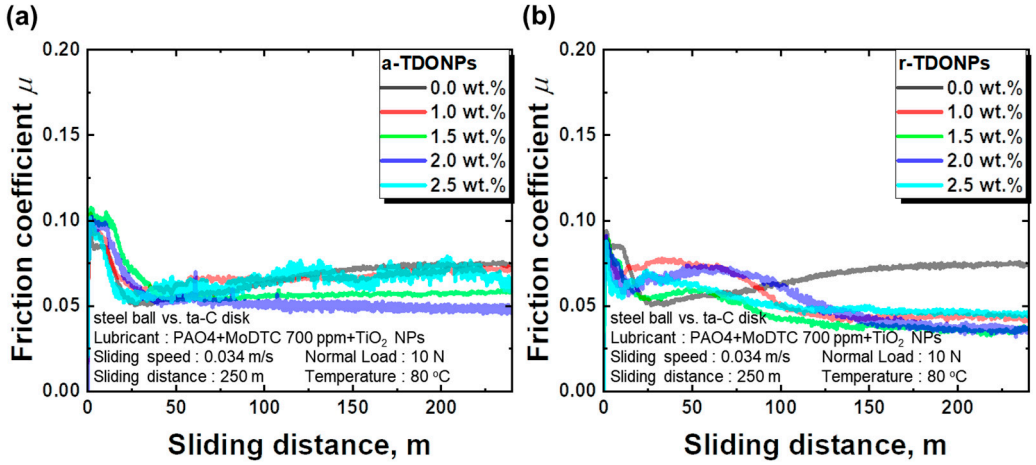

Figure 3. (**a**) Friction curves of ta-C disk/steel ball tribopair under PAO4 mixed with MoDTC 700 ppm and various addition amounts of TDONPs: (**a**) a-TDONPs and (**b**) r-TDONPs.

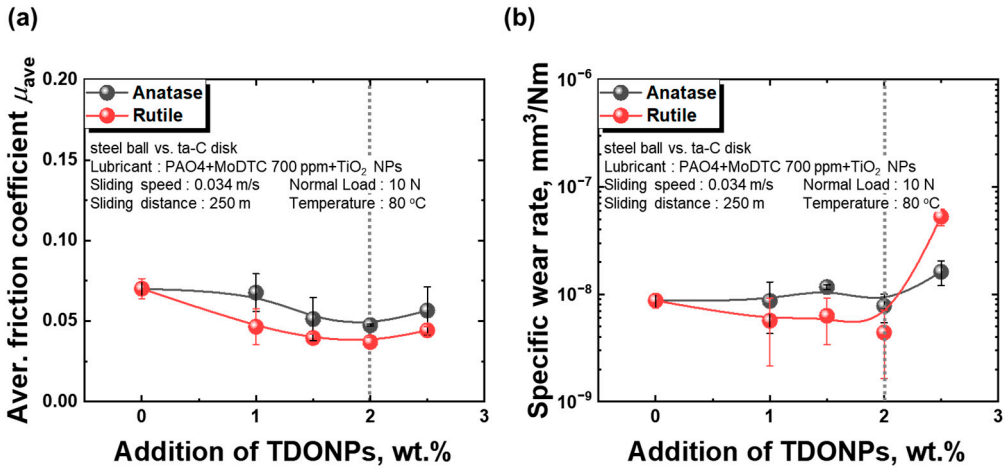

Figure 4. (**a**) Average friction coefficient for steady-state (240–250 m) and (**b**) specific wear rate of ta-C disk under PAO4 mixed with MoDTC 700 ppm and various addition amounts of TDONPs.

Figure 5 shows images of the worn surface of the ta-C disk and steel ball with increasing a-TDONPs loading. Tribofilm was hardly formed on ta-C under MoDTC-containing PAO4 without TDONPs addition. It was also observed that friction by-products in the form of islands were attached to the steel ball. Instead of being in the shape of a complete film, the triboproduct was formed in the form of scattered islands before the evolution to a tribofilm. Compared to the ball, it can be seen that the triboproduct was formed in dots here and there rather than covering the surface, and it was concentrated in the middle of the wear track. However, as the addition of TDONPs increased, island-like triboproducts gradually formed on ta-C, and island-like products gradually developed in the form of films on steel balls. The development of the tribofilm that appeared along with lowering the friction is thought to be the cause of the friction reduction. In the case of r-TDONPs, more products were attached to the ta-C disk. It is assumed that TDONPs contributed greatly to developing the tribofilm and low friction.

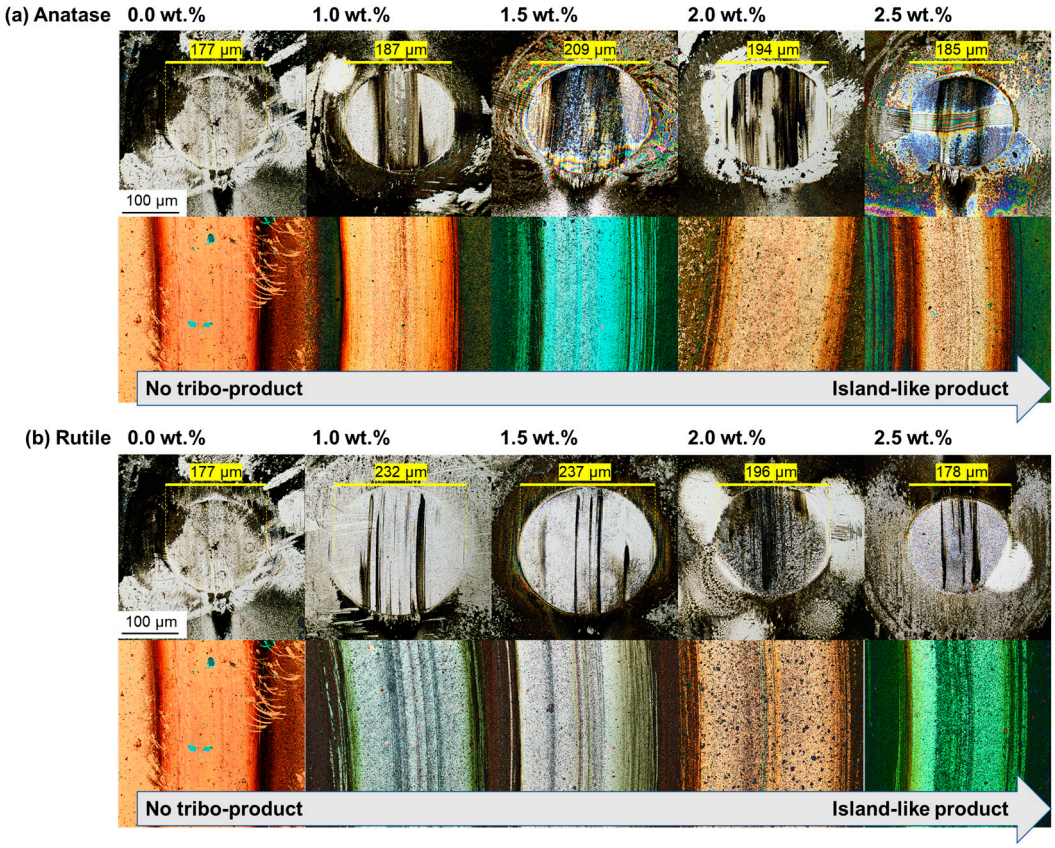

Figure 5. Optical images of wear track on ta-C disk and wear scar of steel ball after friction test under PAO4 mixed with MoDTC 700 ppm and TDONPs: (**a**) a-TDONPs and (**b**) r-TDONPs.

Both a-TDONPs and r-TDONPs showed the highest wear scar diameter (WSD) when 1.5 wt.% was added; however, it gradually decreased as the addition amount of TiO_2 NPs increased beyond 1.5 wt.%. This phenomenon is attributed to the three-body abrasion effect of nanoparticles at concentrations below 1.5 wt.%, leading to an increased WSD of the steel ball. Conversely, at concentrations above 1.5 wt.% of TiO_2 NPs, the formation of a soft MoDTC-based tribofilm prevented direct contact between the ball and ta-C, thereby reducing the WSD. Additionally, the rutile phase showed a higher WSD of the steel ball, which is likely due to its higher hardness compared to anatase, resulting in more severe three-body abrasion.

Representatively, the composition of the tribofilm formed under the addition of 0.0 wt.% and 2.0 wt.% of a-TDONPs or r-TDONPs was investigated by using EDS (Figure 6). Since the EDS energy levels of Mo *L* and S *K* are similar, it is difficult to distinguish them, so they were not divided. As a result, when a-TDONPs were not added, Mo or S signals were mainly detected outside the wear track on ta-C. In contrast, when 2.0 wt.% of aTDONPs was added, Mo or S signals were also strongly detected in the center of the wear track on ta-C. Moreover, in r-TDONPs, Mo or S intensity was obtained extensively inside the wear track of ta-C. The friction coefficient gradually decreased as the formation area of the tribofilm containing Mo or S increased on the ta-C disk. The addition of TDONPs could form MoDTC-derived tribofilms on the ta-C disk, and their effects were different for each phase of TiO_2. On the other hand, a Ti interlayer was deposited to increase ta-C adhesion; therefore, no significant difference could be obtained in the Ti mapping result. On the surface of the steel ball, the Mo or S intensity was detected weakly and narrowly under lubrication without TDONPs addition. On the other hand, under the lubricant added with 2.0 wt.% of a-TDONPs or r-TDONPs, the intensity of Mo or S inside the worn surface was higher than that outside the worn surface on the steel ball. At the same time, Ti was detected at the same location as Mo or S. This might suggest that Ti, which we intended,

played a role as the adhesive layer of tribofilm. Based on the results so far, it was deduced that Ti increased the adhesion of Mo-or S-containing tribofilms. Their chemical structures are covered in Section 3.2 below.

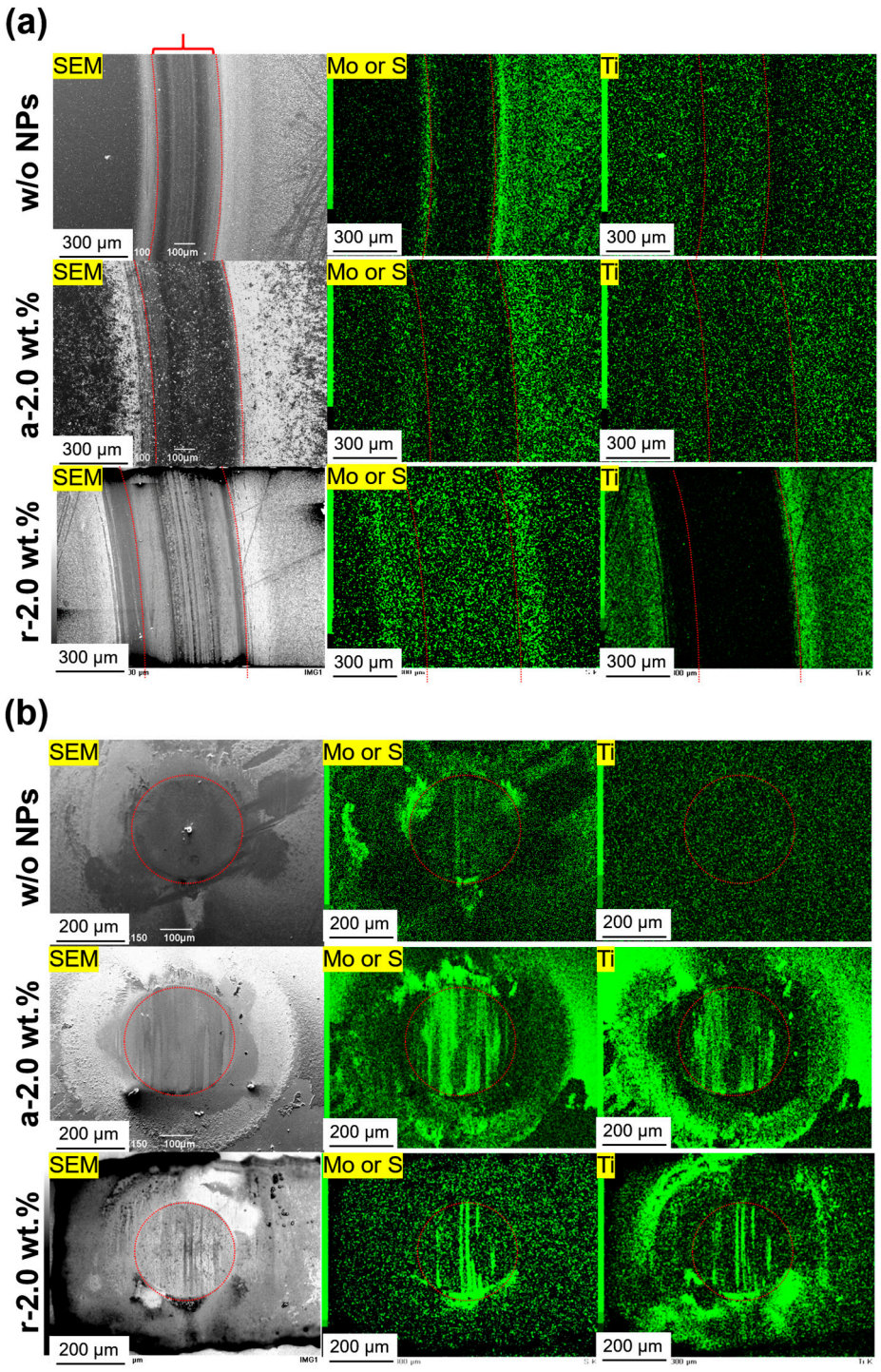

Figure 6. Images of SEM and EDS mapping on (**a**) ta-C disk and (**b**) steel ball. w/o NPs, a—2.0 wt.%, r—2.0 wt.% indicate worn surfaces lubricated under without NPs, and with 2 wt.% of a-TDONPs and r-TDONPs.

3.2. Chemical Structure of Tribofilm

We tried to reveal the chemical structure of friction by-products using Raman spectroscopy. In Raman spectra, all tribosurfaces were carbon-containing structures, and we focused on the spectral range of 100–1100 cm^{-1} with the peaks of anatase- and rutile-phase

TiO_2 [23], Fe_2O_3 [24], MoS_2 [25], Ti-FeO_x [26,27], and MoO_3 [28]. Island-like triboproducts were formed on the surface of the steel ball under lubrication without adding TDONPs. Raman spectra were obtained as shown in Figure 7a, where the triboproduct was generally sparse and loose in area (2). All of them contained MoS_2, and some contained MoO_3 as well. Also, oxides of Fe_2O_3 were strongly detected in the region (1). In contrast, the formation of a relatively thick and wide tribofilm was confirmed under a lubricating environment in which 2 wt.% of a-TDONPs were added. There was no significant difference in the structure measured for the thick and densely formed tribofilm (3) and the thin and sparsely formed area (4). In the case of r-TDONPs, a thin and narrow tribofilm was formed on the worn surface (5, 6). In the tribofilm formed on steel balls lubricated with TDONPs, anatase- and rutile-phase TiO_2 peaks appeared, and additional Ti-substituted phases (denoted as Ti-FeO_x) appeared in the tribofilm. On the other hand, the tribofilm was sparsely formed on the surface without TiO_2, as if the adhesion was insufficient. Therefore, it could mean that Ti is strongly chemically bonded to Fe. It is inferred that MoS_2 was formed on a chemically bonded TiO_2 surface.

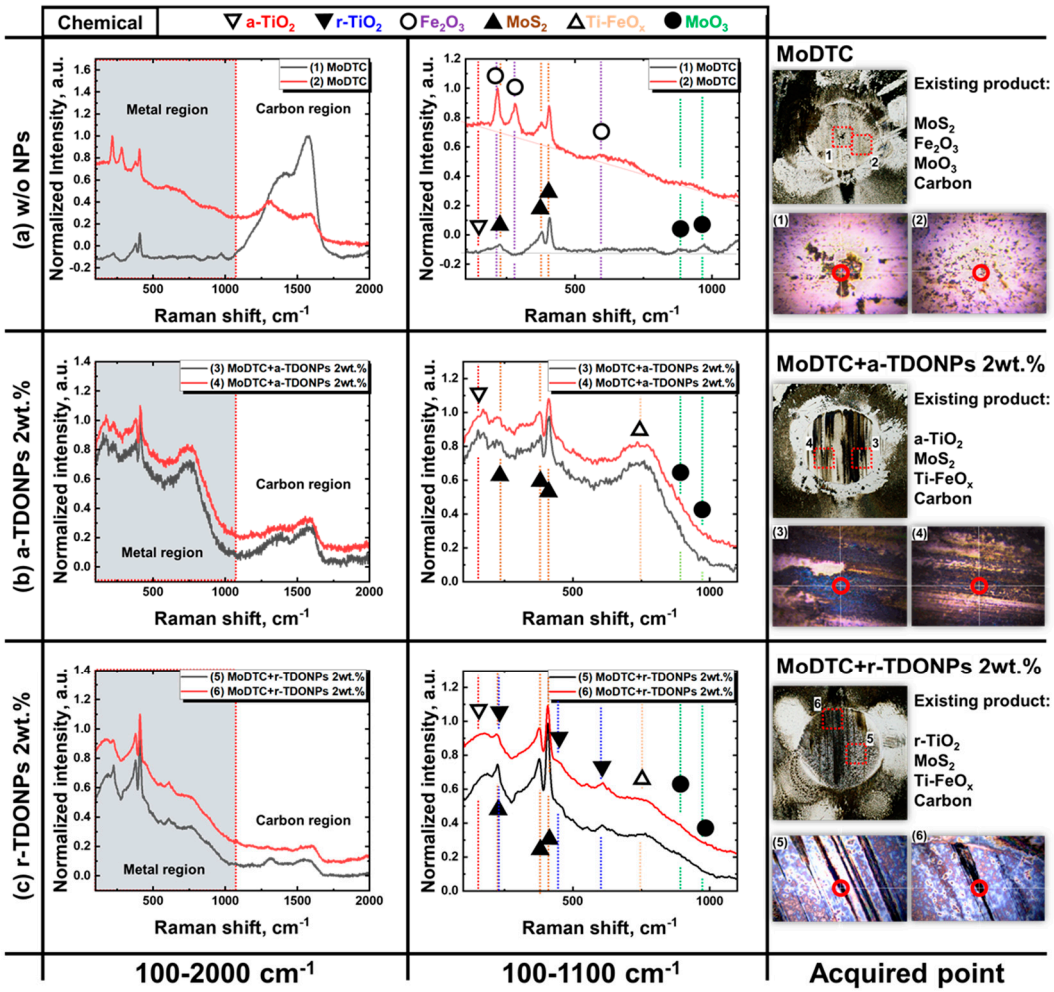

Figure 7. Raman spectra of tribofilm formed on the worn surface of steel ball: (**a**) without NPs, and with (**b**) a-TDONPs 2 wt.% or (**c**) r-TDONPs 2 wt.%. Red-colored circles indicate acquired points.

Finally, no Mo-based peaks appeared on ta-C under lubrication without adding TDONPs (Figure 8). However, when 2 wt.% of a-TDONPs or r-TDONPs were added, TiO_2 and MoS_2 peaks appeared on ta-C simultaneously, similar to the steel ball. From this, we could know that titanium assisted the formation of tribofilm on the chemically stable ta-C surface.

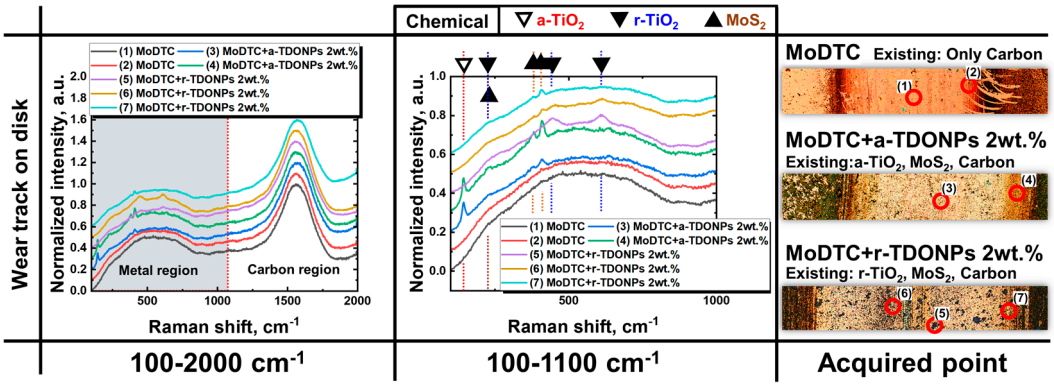

Figure 8. Raman spectra of tribofilm formed on worn surface of ta-C disk. Red-colored circles indicate acquired points.

The element ratio and bonding state of each tribofilm were confirmed using XPS. The spectra of Ti 2*p*, S 2*p*, and Mo 3*d* were obtained, and details of each fit with the Gaussian–Lorentzian function can be found in Table 1 [29]. The doublet separation and area ratio of S 2*p*3/2–2*p*1/2 were 1.18 eV with a 2:1 area ratio with equal FWHM. Ti 2*p*3/2–2*p*1/2 was split with 5.7 eV with a 2:1 area ratio and FWHM. The Mo 3*d*5/2–3*d*3/2 splitting was 3.13 eV with a 3:2 area ratio with equal FWHM. Figure 9 displays a representative peak deconvolution.

Table 1. Details of peak fits related to XPS analyses of tribofilm.

Element	Contribution	Binding Energy, eV	Assigned Species	G/L Ratio	Ref.
S 2*p*3/2	S^0	164.0 ± 0.2	S-S/CS_2	2:8	[30]
	$(S_2)^{2-}$	163.4 ± 0.2	MoO_yS_x/MoS_3		[31]
	S^{2-} in Mo-S	162.4 ± 0.2	MoS_2		[31]
Ti 2*p*3/2	Ti^{4+}	458.7 ± 0.3	TiO_2	7:3	[32,33]
	Ti^{3+}	456.5 ± 0.3	TiO_{2-x}		[32]
	Ti^{2+}	455.1 ± 0.3	TiC/TiO		[33,34]
Mo 3*d*5/2	Mo^{6+}	232.6 ± 0.3	MoO_3/MoS_3	2:8	[33,35]
	Mo^{5+}	231.0 ± 0.3	$MoO_x/MoS_x/MoO_yS_x$		[33,36]
	Mo^{4+}	229.4 ± 0.3	MoS_2/MoO_2		[35]
	Mo^{2+}	228.6 ± 0.3	Mo_2C/MoO		[33,35]
	Mo^0	227.8 ± 0.3	Mo-metal		[35]

The additive-derived tribofilm formed on the ta-C disk and steel ball appeared to be in a small amount, and S was detected only on the outermost surface of the tribofilm regardless of the presence or absence of TDONPs; almost no S was detected after 1 min of sputtering (Figures 10 and 11). In addition, the tribofilm formed on the ta-C disk and steel balls lubricated with TDONPs contained Mo, S, O, and Ti together, and as the sputtering time increased, they gradually decreased, and only their base material (i.e., ta-C and SUJ2) was detected after 5 min of sputtering. From this, we were able to obtain information at the interface between the tribofilm and the ta-C disk or the steel ball. Also, the significant difference is that, as shown in Figure 11a, a very thin or small tribofilm was observed on the steel ball rubbed without TDONPs.

Mo^{5+} and Mo^{6+} bonds gradually decreased from the surface to the bulk direction, and the intensity of Mo^{2+} increased on the ta-C disks (Figure 12). Additionally, when lubricated with TDONPs, the intensity of Mo^0 also increased in the tribofilm formed on the ta-C disks, suggesting that Mo formed a metallic bond with Ti. On the other hand, no notable change in area ratio was observed in the tribofilm formed on the steel ball in Mo3*d* (Figure 13). In Ti 2*p* spectra, Ti^{4+} was dominant on the surface, and the Ti^{4+} area ratio decreased toward the interfaces between the tribofilm/ta-C disk and the tribofilm/steel ball (Figures 12 and 13). Unfortunately, for the ball lubricated without TDONPs, the element S was not detected after pre-sputtering to remove the residual oil. Furthermore, MoS_2 (Mo^{4+})

and MoO_3 (Mo^{6+}), which were found in the Raman spectra, were barely observed after peak deconvolution in the XPS spectra. This is likely the result of a thin tribofilm forming on the balls as shown in Figure 7, which disappeared after a short pre-sputtering. The results of peak deconvolution also explain why the MoDTC-derived tribofilm adhered well under TDONPs lubrication. The tribofilm on ta-C showed an increase in Ti^{2+}, which appeared to be the result of carbide formation where Ti combines with C (Figure 12d,e). On the other hand, in the tribofilm formed on the steel ball, only the Ti^{3+} intensity increased without an increase in the Ti^{2+} fraction (Figure 13d,e). The increase in Ti^{3+} in the tribofilm formed on the steel ball is thought to represent the Raman vibration in Ti-FeO_x. In addition, it was shown that the Ti/Mo atomic ratio in the tribofilm formed on ta-C disk increased with an increasing sputtering time (Figure 14a). From this, it was deduced that Ti, which easily adhered to carbon, preferentially formed a tribofilm, and a tribofilm derived from MoDTC was formed after the formation of an adhesive layer of Ti. From this, it is speculated that the existence of MoS_2 on ta-C in EDS and Raman is due to the formation of the Ti adhesion layer. On the other hand, there was no clear difference in the Ti/Mo element ratio on the steel ball, which might mean that Ti and Mo were mixed in the film at almost similar ratios along the depth direction (Figure 14d). When lubricated without TDONPs, Mo attaches by directly combining with C to form chemical bonds; however, Mo_2C has a higher Gibbs free energy for carbide formation than TiC, which might make it more unstable and result in lower adhesion on the ta-C disk (Figure 14b). On the other hand, ta-C lubricated in TDONPs can be rigidly attached to the chemically stable ta-C due to the strong bonding of TiC, so that MoDTC-derived tribofilms could be stably produced. In particular, the increase in Ti^{3+} seen in both the ball and the disk is believed to have contributed to the creation of these products and is discussed in Section 3.4.

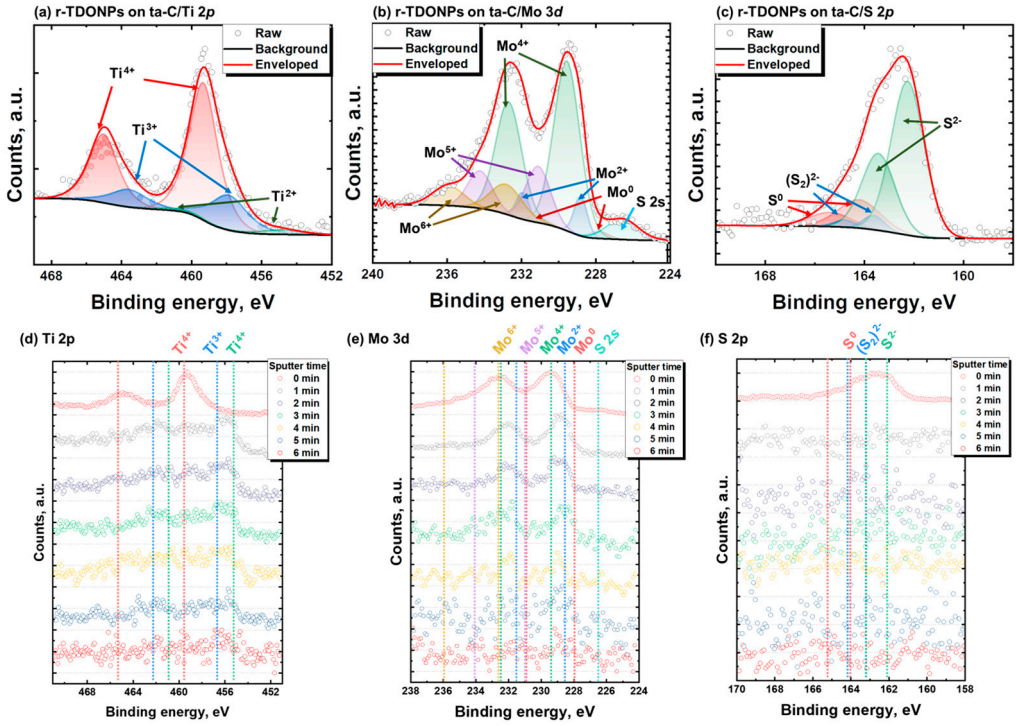

Figure 9. Respective XPS spectra for (**a**) Ti 2*p*, (**b**) Mo 3*d*, and (**c**) S 2*p* of worn surface on ta-C disks under PAO4 oil with 2 wt.% r-TDONPs and 700 ppm MoDTC. Depth profiling XPS analysis for (**d**) Ti 2*p*, (**e**) Mo 3*d*, and (**f**) S 2*p* of tribofilm formed on ta-C slid under 2 wt.% r-TDONPs containing MoDTC lubricant.

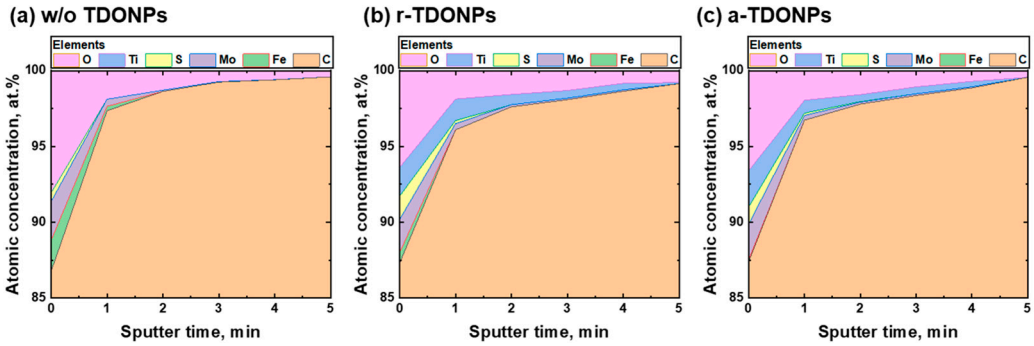

Figure 10. Depth profile of atomic concentration of tribofilms on ta-C disks lubricated without (**a**) TDONPs, and with 2 wt.% of (**b**) r-TDONPs and (**c**) a-TDONPs.

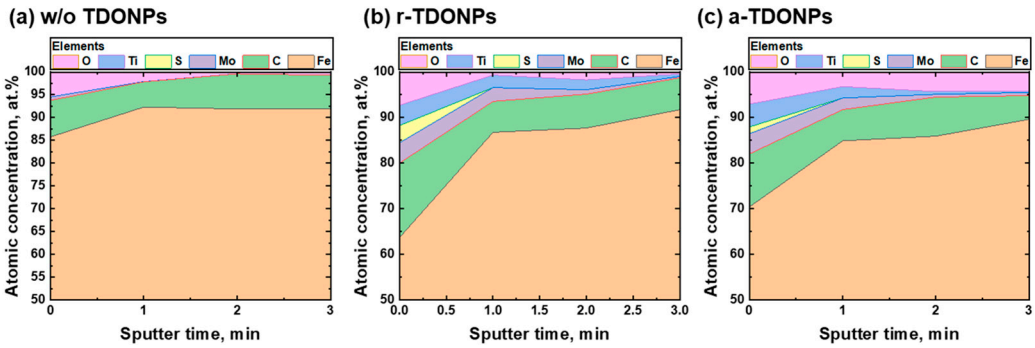

Figure 11. Depth profile of atomic concentration of tribofilms on steel balls lubricated (**a**) without TDONPs, and with 2 wt.% of (**b**) r-TDONPs and (**c**) a-TDONPs.

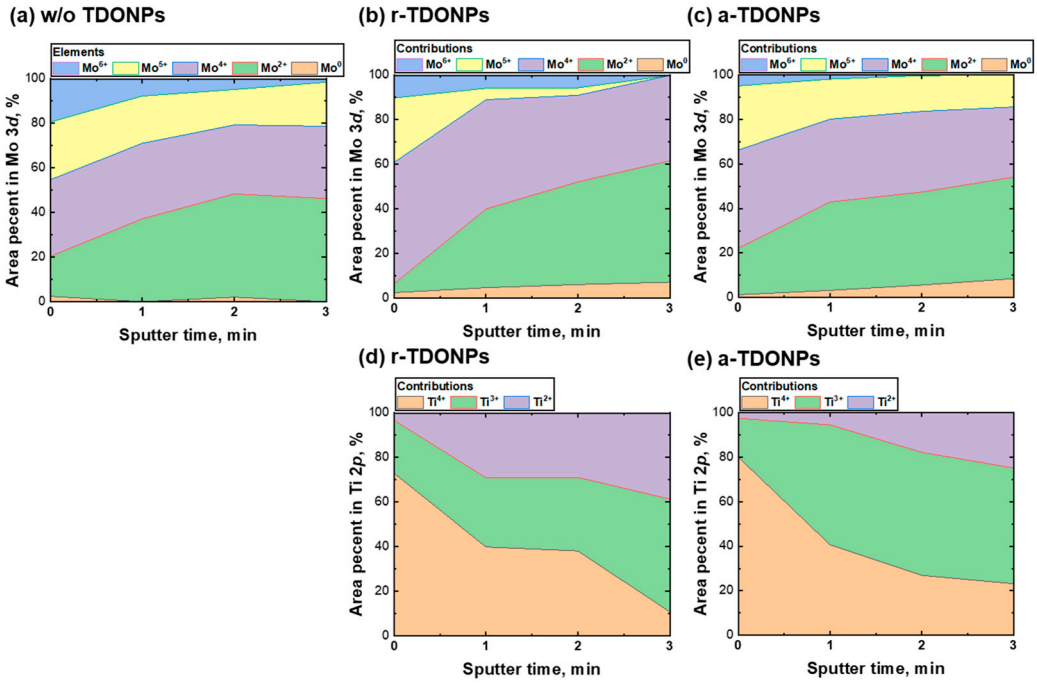

Figure 12. Area percent in (**a**–**c**) Mo 3*d* and (**d**,**e**) Ti 2*p* of tribofilms on ta-C disks: (**a**) without TDONPs, (**b**,**d**) with r-TDONPs 2 wt.%, and (**c**,**e**) with a-TDONPs 2 wt.%.

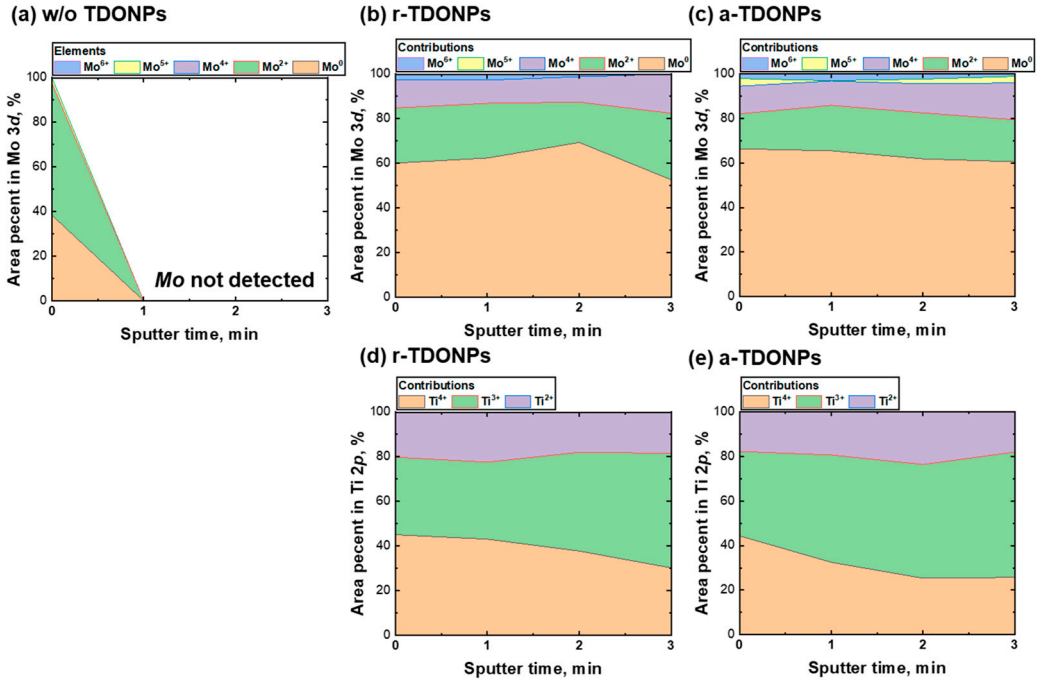

Figure 13. Area percent in (**a**–**c**) Mo 3*d* and (**d**,**e**) Ti 2*p* of tribofilms on steel balls: (**a**) without TDONPs, (**b**,**d**) with r-TDONPs 2 wt.%, and (**c**,**e**) with a-TDONPs 2 wt.%.

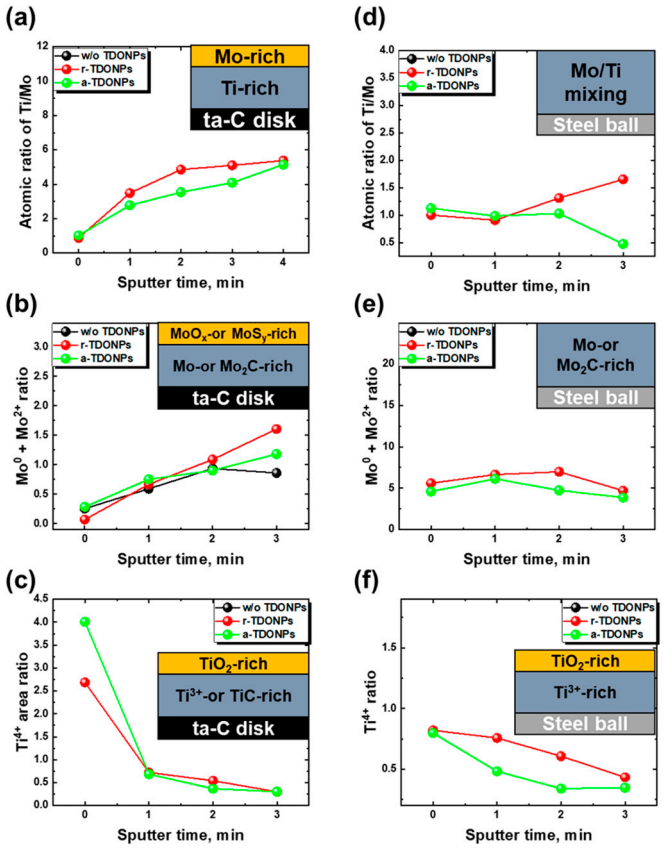

Figure 14. Atomic ratio of (**a**,**d**) S/Mo, (**b**,**e**) area ratio of Mo^0 and Mo^{2+} in Mo 3*d*, and (**c**,**f**) Ti^{4+} in Ti 2*p* in tribofilm: (**a**–**c**) ta-C disks and (**d**–**f**) steel balls.

Figure 15 shows the XPS spectra on surfaces on ta-C. The Mo^{4+} and S^{2-} intensities were higher on the tribosurface rubbed with r-TDONPs. Figures 16 and 17 show the atomic concentration and bonding percentage of tribofilm formed on the outermost surface of

the ta-C disk and steel ball. When TDONPs were not added, there was relatively little Mo^{4+} in Mo 3*d* and S^{2-} in S 2*p* in the tribofilm formed on the ta-C disk. Moreover, there was almost no Mo^{4+} on the steel ball, and S was not detected either. This suggests that the content of MoS_2 on its surfaces lubricated without TDONPs was lower than that on surfaces lubricated with TDONPs. In addition, the elemental ratio of S/Mo and S/O, and the bonding ratio of Mo^{4+} in Mo 3*d* are shown in Figures 16e and 17e. Their ratio suggests that r-TDONPs are the superior additive for both steel balls and ta-C disks. Figure 18 shows their relationship with the friction coefficient. They show strong agreement with the low friction under TDONPs-containing lubricating oil, which is attributed to the low friction properties due to the MoS_2-rich tribofilm formed on the outermost surface.

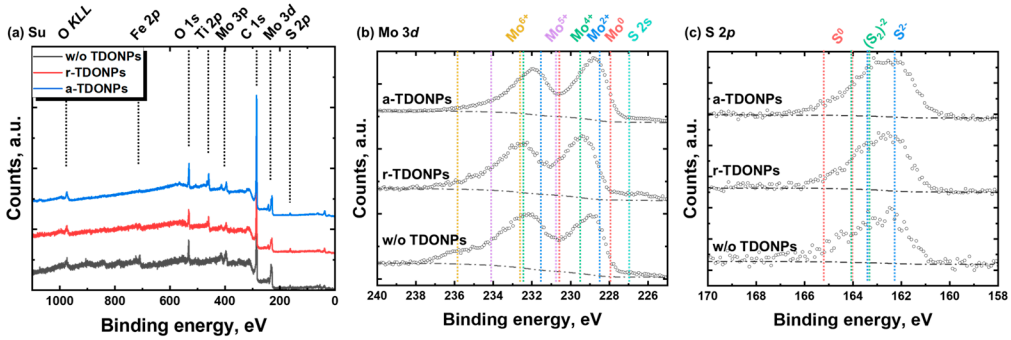

Figure 15. XPS spectra for (**a**) survey, (**b**) S 2*p*, and (**c**) Mo 3*d* of worn surface on ta-C disks lubricated without TDONPs and with a-TDONPs and r-TDONPs.

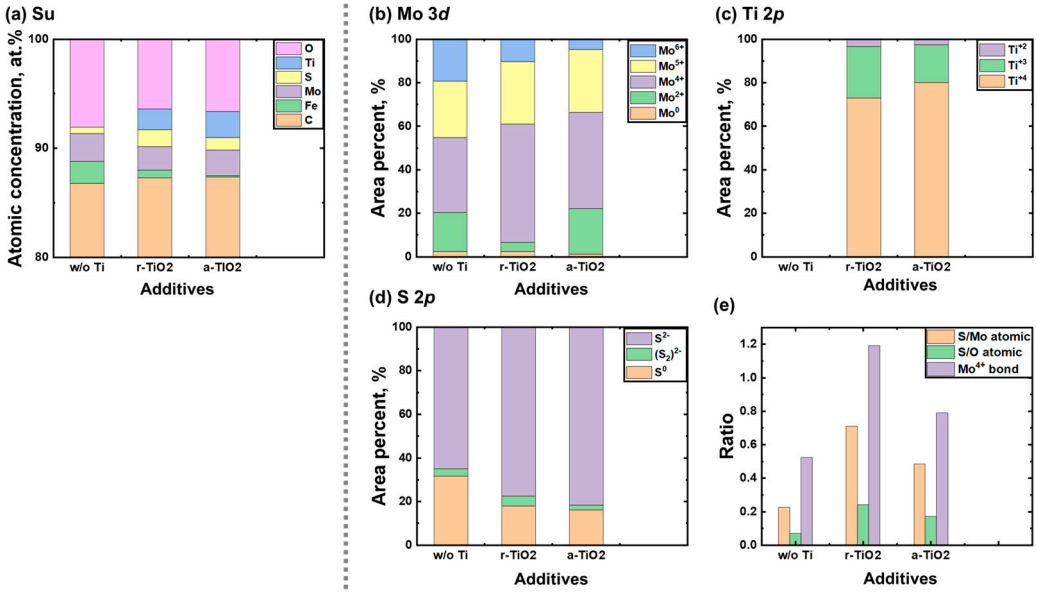

Figure 16. (**a**) Atomic concentration of worn surface on ta-C disks and area percent in (**b**) Mo 3*d*, (**c**) Ti 2*p*, and (**d**) S 2*p* lubricated without TDONPs, and with 2 wt.% of r-TDONPs and a-TDONPs. (**e**) Atomic ratio of S/Mo and S/O, and bonding ratio of Mo^{4+} of worn ta-C disks.

After lubricating without TDONPs, additives-derived tribofilm formed little on both the ta-C disk and steel ball. Moreover, Mo oxide was formed on ta-C lubricated without TDONPs mainly compared to low-shearing MoS_2. On the other hand, in the case of the addition of 2 wt.% of TDONPs, Mo and S were adhered on the ta-C disk with a TiC carbide bond. Comparing S 2*p* and Mo 3*d*, the MoS_2 content of tribofilm slid under 2 wt.% of TDONPs lubricant was higher than that which slid with 0 wt.% of TDONPs. Onodera et al. [37] reported that MoDTC transformed into a bridging isomer of MoDTC (Li-MoDTC) at moderate temperatures. Deshpande et al. [38,39] reported that the decomposition of MoDTC was accelerated by the catalysis of a TiO_2 atmospheric plasma-spray coating.

Likewise, the degradation of MoDTC by r-TDONPs and a-TDONPs assisted in the sustained formation and lubrication of MoS_2 tribofilms. On the other hand, when TDONPs were not added, the MoS_2 formation rate was significantly lower than the oxidation rate, making it difficult to maintain the MoS_2-based contact interface. Thus, TDONPs are expected to be useful for the decomposition of MoDTC and the adhesion of MoS_2-derived tribofilms. Moreover, it is suggested that a ta-C disk lubricated with lubricants added with TDONPs formed a Mo-Ti metallic bond and TiC carbide bond on the ta-C disk, which further attracted the tribofilm and led to the interlaminar shear properties of MoS_2. Galhenage et al. [40] conducted a computational study based on density functional theory on the growth of MoS_2 on TiO_2 as to why TiO_2 exhibited a strong interaction with MoS_2. It was found that strong covalent bonds were formed by preferentially coordinating the bridging O atoms in TiO_2 to the edge S atoms of MoS_2. These studies explain why TDONPs persisted and formed well on MoDTC-derived tribofilms.

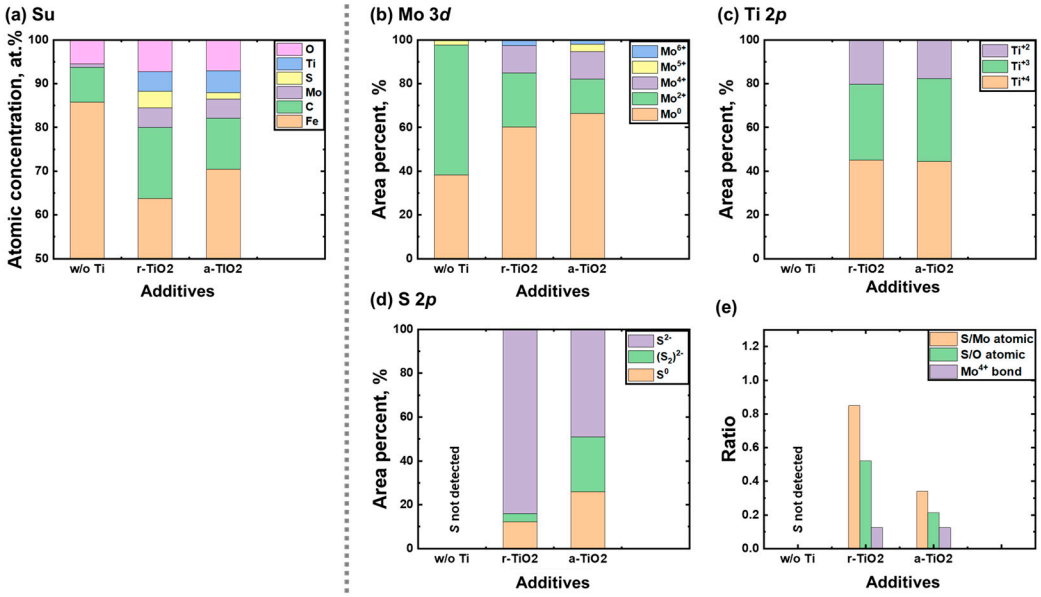

Figure 17. (**a**) Atomic concentration of worn surface on steel balls and area percent in (**b**) Mo 3*d*, (**c**) Ti 2*p*, and (**d**) S 2*p* lubricated without TDONPs, and with 2 wt.% of r-TDONPs and a-TDONPs. (**e**) Atomic ratio of S/Mo and S/O, and bonding ratio of Mo^{4+} of worn steel balls.

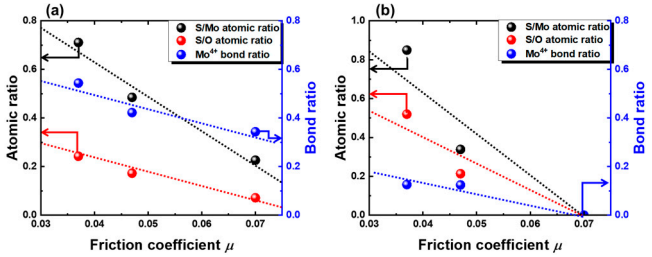

Figure 18. Relationship between friction coefficient and atomic ratio of Mo/S and O/S and bonding ratio of Mo^{4+}: (**a**) ta-C disk and (**b**) steel ball.

3.3. Friction Performance of TiO_2 Nanoparticles without Light

Since TDONPs are used as an excellent photocatalyst, to determine the effect of light energy, a light and dark environment was created in the tribometer system using LEDs and a blackout curtain, respectively. A blackout curtain was installed surrounding the tribometer, and the LED was irradiated directly to the specimen. The experimental conditions of the tribotest were the same as in the previous section, with the addition of 2 wt.% a-TDONPs, which was the most efficient photocatalyst among TiO_2. Figure 19 shows the effect of light energy on the friction characteristics to clarify the photocatalytic influence. The dark and

bright environments showed similar friction coefficients of 0.053 and 0.048, and their wear rates showed little difference within the error bar range. The friction coefficient showed a slight difference of approximately 0.005 in a dark environment, and it was confirmed that the friction reduction was not a photocatalytic effect.

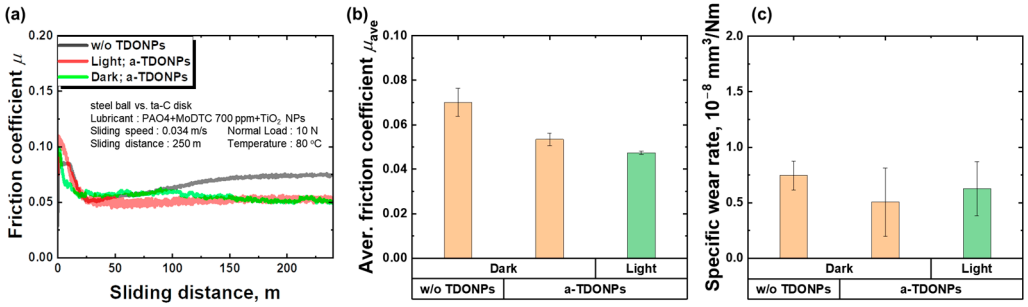

Figure 19. (**a**) Friction curves, (**b**) average friction coefficient, and (**c**) specific wear rate of ta-C under PAO4 mixed with MoDTC 700 ppm and 2 wt.% a-TDONPs.

3.4. Friction Performance of TiO_2 Nanoparticles without MoDTC Addition

In addition to MoDTC, OA generally exhibits excellent low friction when used as a lubricant, so we sought to investigate the friction reduction effect of OA without an MoDTC addition. We added 0, 1, and 2 wt.% of a-TDONPs to PAO4 to investigate only the characteristics of OA-modified a-TDONPs. The tribological properties of the ta-C/steel tribopair were evaluated under a load of 10 N, a speed of 34 mm/s, and at room temperature for 3 h. The Lambda ratio at the beginning of the friction was 0.26, which was lubrication belonging to the boundary lubrication regime. Further, we aimed to investigate whether a-TDONPs adhere to ta-C and steel without additional thermal energy under boundary lubrication.

Figure 20 shows the friction curve and the average CoF during a steady state. In the absence of MoDTC, the friction-reducing effect of a-TDONPs was not significantly different. Pure PAO4 showed a coefficient of friction of 0.077, and even when 2 wt.% of a-TDONPs was added, the CoF was almost similar to 0.075. Therefore, the tribological performance could not be improved only by the addition of a-TDONPs. Conventionally, friction reduction mechanisms by the mechanical movement of NPs such as rolling, sliding, and exfoliation are reported [41]. On the other hand, in this study, such an effect was not seen, and the friction reduction by simply adding nanoparticles could not be expected. In addition, OA also acts as an additive or lubricant contributing to low friction; however, the friction reduction caused by OA was not shown in OA-modified a-TDONPs-containing lubricant.

To confirm that the a-TDONPs formed any additional friction by-products, we observed wear scars on the steel balls. Figure 21a shows an optical image of the worn surface of a steel ball slit under lubricant without TDONPs. A black-colored tribofilm was observed in the optical images of balls lubricated in pure PAO4. On the other hand, when a-TDONPs were added, it was confirmed that a blue tribofilm was gradually formed. Therefore, it was found that additional triboproducts were formed when lubricated with a-TDONPs. Figure 21b shows EDS mapping images of balls lubricated in PAO4 with 0 wt.% and 2 wt.% of a-TDONPs. In the case of ta-C, no difference was observed because the Ti interlayer was used to increase ta-C adhesion. The black tribofilm formed under pure PAO4 lubrication was mostly composed of iron and oxygen, whereas the blue tribofilm formed with the addition of TDONPs was composed of carbon, titanium, and oxygen. The black tribofilm was composed of iron oxide, and the blue tribofilm was estimated to be composed of titanium carbide, titanium oxide, and free carbon.

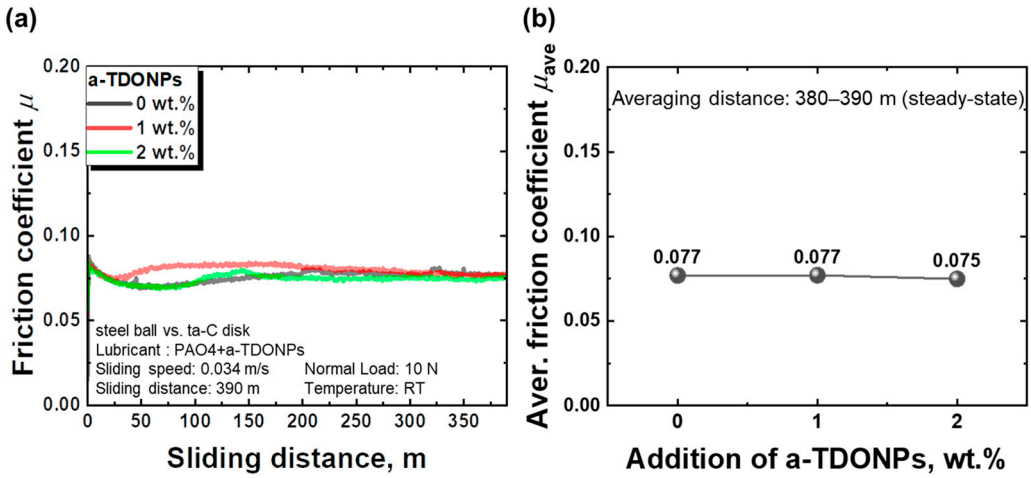

Figure 20. (**a**) Friction curves and (**b**) average friction coefficient for steady-state ta-C disk/steel ball tribopair under PAO4 with various addition amounts of a-TDONPs.

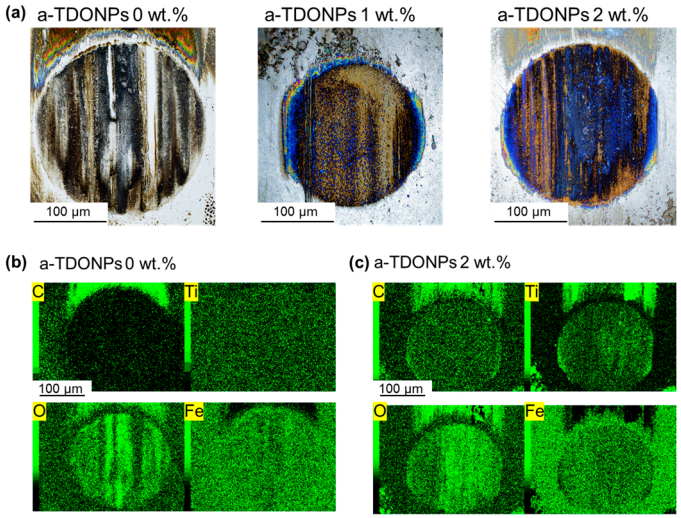

Figure 21. (**a**) Optical images and (**b**,**c**) EDS mapping images of wear scar on steel ball lubricated under PAO with various addition amounts of a-TDONPs.

As shown in Figure 22, the atomic ratio of Ti/C in the depth direction of the tribofilm gradually increased in the steel ball and gradually decreased in the ta-C disk. Therefore, it can be seen that a-TDONPs adhere well to the surfaces of the steel ball and ta-C disk. Vengudusamy et al. [8] reported that the friction did not significantly decrease under PAO4 lubrication at the C/C contact interface using various types of self-mated DLCs. Comparing their work, it is understandable that the friction did not decrease despite the formation of carbonaceous tribofilms. We reported in a previous study that when titanium is attached to a mating material, it serves as an adhesive layer and improves the adhesion of tribofilm [15,16,42]. Therefore, it is assumed that the addition of a-TDONPs caused titanium to adhere onto iron and strongly attract carbon. Finally, we could expect the desired adhesion of Ti and the catalytic effect of TiO_2.

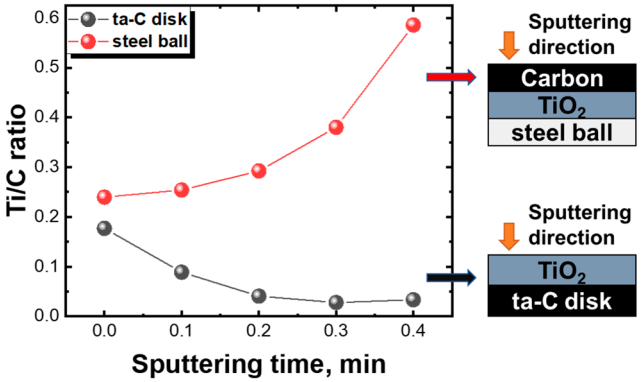

Figure 22. Ti/C atomic ratio measured using AES of tribofilm in depth direction on a steel ball and ta-C disk.

4. Discussion

A MoDTC-based tribofilm does not form well on general DLC. Doping metal into the DLC matrix can form a MoDTC-based friction film; however, metal doping has the problem of deteriorating the mechanical properties of DLC [7–9]. We added TiO_2 to the oil to improve the friction properties under MoDTC-added oil without deteriorating the mechanical properties of DLC, and, as a result, we were able to form a MoDTC-based tribofilm on DLC. The friction reduction effectiveness of TiO_2 NPs has been previously reported under water lubrication [43,44]. On the other hand, there have been few comparisons between anatase and rutile phases, and the friction reduction effect was reported only for the steel/steel tribopair. MoDTC is known to decompose by electron transfer to form MoS_2 [45]. Deshpande et al. [38,39] deduced that electrons emitted by the photocatalytic properties of TiO_2 as an n-type semiconductor could break the bond of MoDTC. On the other hand, the photocatalytic properties of TiO_2 are superior in the anatase phase compared to the rutile phase [46]. In this study, the decomposition of MoDTC in rutile-phase TDONPs and the formation of a MoS2-containing tribofilm were effective. Kajdas and Hiratsuka [47–49] reported that tribochemistry or tribocatalysis is related to a 'negative-ion-radical action mechanism'. The emitted electrons, which are composited of exoelectrons and thermal electrons, act with lubricant molecules and decompose the lubricant. The neutral atoms or molecules cause an anti-emission with electron absorption and hurt the triboemission, considered from 'intermediate excited states', which mechano-chemically influence the dissolution of chemical bonds. Hence, excited states of the nascent surface involve the emission of electrons, ions, molecules, and so on, and charged electrons and ions could have a positive effect on the triboemission [50]. This phenomenon helps us understand the formation of a MoDTC-derived tribofilm on an oxide layer or a non-metallic surface formed during the rubbing of metallic bulk material. [51,52]. It is often reported that the decomposition of MoDTC and the formation of a MoS_2 tribofilm are formed on iron oxide or a chrome oxide tribolayer [53], and we believe this is due to such triboemission properties. Fan et al. [54] also focused on the fact that tribocatalysts could be operated by tribocharing or triboelectrification. The exoelectron and thermionic emission are related to the Seebeck effect, and a triboelectric charge was recently reported through this relationship [55]. Upon contact and release of DLC and TDONPs, electrons might move due to triboelectric charge, which can be evaluated by the triboelectric factor ξ:

$$\xi = S/\sqrt{\rho c k} \quad (1)$$

where, S, ρ, c, and k are the Seebeck coefficient, material density, specific heat, and thermal conductivity. The triboelectric factor of rutile (−0.154–−0.079) is quite high compared to that of anatase (−0.102–−0.049). As r-TDONPs are rubbed with DLC, electrons are transferred to DLC, and it is believed that these released electrons can help decompose MoDTC.

The adhesive and catalytic properties of Ti are shown in Figure 23. MoDTC is known to be decomposed by electrons with alternative switching between Ti^{4+} and Ti^{3+} to form MoS_2-based tribofilms in the following:

$$Ti^{4+} + e_{CB}{}^{-} + \text{LI-MoDTC}\ (Mo_2O_2S_2\ [R_2NCS_2]_2) \rightarrow Ti^{3+} + 2MoS_2 + 2R_2NCOS \quad (2)$$

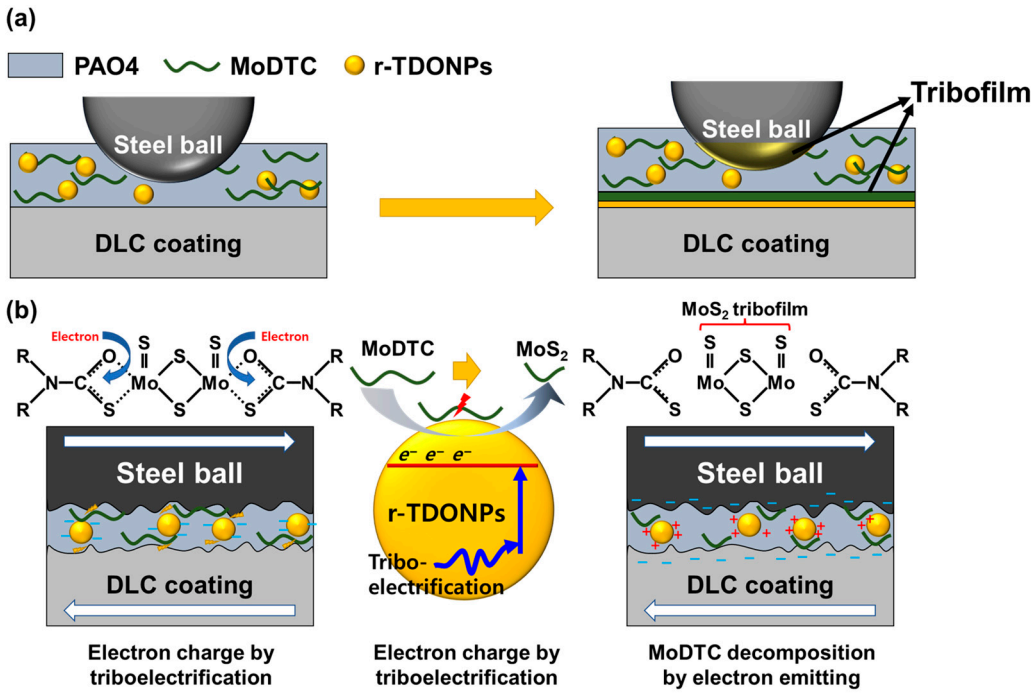

Figure 23. Schematic of (**a**) the expected tribofilm structure and (**b**) degradation of MoDTC with TDONPs.

The *d*-vacancies of Ti lead to chemical bonding and are preferentially adhered to the surface of the ta-C disk and steel ball to form a robust adhesive layer. After that, the TDONPs are activated due to the frictional energy and expel electrons into LI-MoDTC, which decomposes MoDTC into MoS_2. As a result, the MoDTC-derived tribofilm is strongly adsorbed on the contact surface to form a MoS_2/MoS_2 contact interface, resulting in low friction.

5. Conclusions

In this study, TDONPs were dispersed in MoDTC-containing lubricating oil to improve tribological performance through their catalytic and reactive properties. We tried to exclude the effects of light irradiation and oleic acid to clearly identify the effects of TDONPs. The key findings are summarized as follows:

(1) TDONPs alone added to PAO4 lubricant without MoDTC did not improve the friction performance. On the other hand, TDONPs attached to the wear surface of DLC and steel activated the surface to attach carbon.

(2) Dispersion of the TDONPs in PAO4 oil containing MoDTC improved the lubrication performance by up to ~100%. When a-TDONPs were added at 1 wt.% and 2.5 wt.%, the effect of reducing friction was not significant. The optimal content of TDONPs was 2.0 wt.%, and when more than this was added, the friction and wear increased due to a rapid decrease in precipitation and dispersion performance.

(3) The addition of TDONPs may have increased the formation or adhesion of MoS_2 on the DLC and steel surfaces, thereby reducing friction.

(4) The improved friction and wear characteristics of r-TDONPs were superior to those of a-TDONPs, and this difference in tribocatalytic properties is presumed to result from their triboelectric capabilities.

(5) TDONPs have been tribologically useful additives due to their adhesive and catalytic action, but the technology to maintain their dispersion remains a problem to be solved.

Author Contributions: Conceptualization, J.-I.K. and N.U.; methodology, J.-H.P. and R.I.; investigation, J.-I.K.; resources, J.-I.K. and N.U.; data curation, D.M.; writing—original draft preparation, J.-I.K.; writing—review and editing, T.T. and W.-Y.L.; supervision, R.I. and N.U.; project administration, N.U.; funding acquisition, N.U. All authors have read and agreed to the published version of the manuscript.

Funding: This work was supported by KAKENHI (grant number JP22KJ1551).

Institutional Review Board Statement: Not applicable.

Informed Consent Statement: Not applicable.

Data Availability Statement: Data are contained within the article.

Conflicts of Interest: The authors declare no conflicts of interest.

References

1. Spikes, H. Friction Modifier Additives. *Tribol. Lett.* **2015**, *60*, 5. [CrossRef]
2. Yamamoto, Y.; Gondo, S. Friction and Wear Characteristics of Molybdenum Dithiocarbamate and Molybdenum Dithiophosphate. *Tribol. Trans.* **1989**, *32*, 251–257. [CrossRef]
3. Kassim, K.A.M.; Tokoroyama, T.; Murashima, M.; Umehara, N. The Wear Classification of MoDTC-Derived Particles on Silicon and Hydrogenated Diamond-like Carbon at Room Temperature. *Tribol. Int.* **2020**, *147*, 106176. [CrossRef]
4. Kassim, K.A.M.; Tokoroyama, T.; Murashima, M.; Lee, W.Y.; Umehara, N.; Mustafa, M.M.B. Wear Acceleration of A-C:H Coatings by Molybdenum-Derived Particles: Mixing and Temperature Effects. *Tribol. Int.* **2021**, *159*, 106944. [CrossRef]
5. Bin Mustafa, M.M.; Umehara, N.; Tokoroyama, T.; Murashima, M.; Shibata, A.; Utsumi, Y.; Moriguchi, H. Effect of Pillar and Mesh Structure of Tetrahedral Amorphous Carbon (TA-C) Coatings on the Wear Properties and Fracture Toughness of the Coating. *Tribol. Online* **2019**, *14*, 388–397. [CrossRef]
6. Hashizume, N.; Murashima, M.; Umehara, N.; Tokoroyama, T.; Lee, W.-Y. In Situ Observation of the Formation of MoDTC-Derived Tribofilm on a Ta-C Coating Using Reflectance Spectroscopy and Its Effects on Friction. *Tribol. Int.* **2021**, *162*, 107128. [CrossRef]
7. Miyake, S.; Saito, T.; Yasuda, Y.; Okamoto, Y.; Kano, M. Improvement of Boundary Lubrication Properties of Diamond-like Carbon (DLC) Films Due to Metal Addition. *Tribol. Int.* **2004**, *37*, 751–761. [CrossRef]
8. Vengudusamy, B.; Green, J.H.; Lamb, G.D.; Spikes, H.A. Behaviour of MoDTC in DLC/DLC and DLC/Steel Contacts. *Tribol. Int.* **2012**, *54*, 68–76. [CrossRef]
9. Bae, S.M.; Horibata, S.; Miyauchi, Y.; Choi, J. Tribochemical Investigation of Cr-Doped Diamond-like Carbon with a MoDTC-Containing Engine Oil under Boundary Lubricated Condition. *Tribol. Int.* **2023**, *188*, 108849. [CrossRef]
10. Yu, H.; Fu, J.; Zhu, X.; Zhao, Z.; Sui, X.; Sun, S.; He, X.; Zhang, Y.; Ye, W. Tribocatalytic Degradation of Organic Pollutants Using Fe_2O_3 Nanoparticles. *ACS Appl. Nano Mater.* **2023**, *6*, 14364–14373. [CrossRef]
11. Zhang, Q.; Jia, Y.; Wang, X.; Zhang, L.; Yuan, G.; Wu, Z. Efficient Tribocatalysis of Magnetically Recyclable Cobalt Ferrite Nanoparticles through Harvesting Friction Energy. *Sep. Purif. Technol.* **2023**, *307*, 122846. [CrossRef]
12. Li, X.; Tong, W.; Shi, J.; Chen, Y.; Zhang, Y.; An, Q. Tribocatalysis Mechanisms: Electron Transfer and Transition. *J. Mater. Chem. A* **2023**, *11*, 4458–4472. [CrossRef]
13. Fouts, J.A.; Shiller, P.J.; Mistry, K.K.; Evans, R.D.; Doll, G.L. Additive Effects on the Tribological Performance of WC/a-C:H and TiC/a-C:H Coatings in Boundary Lubrication. *Wear* **2017**, *372*, 104–115. [CrossRef]
14. Miyake, S.; Shindo, T.; Suzuki, M. Nanomechanical and Boundary Lubrication Properties of Titanium Carbide and Diamond-like Carbon Nanoperiod Multilayer and Nanocomposite Films. *Surf. Coat. Technol.* **2013**, *221*, 124–132. [CrossRef]
15. Kim, J.I.; Lee, W.Y.; Tokoroyama, T.; Umehara, N. Long-Term Low-Friction of Ti-Overcoated and-Doped DLCs: Robustly Developed Carbonous Transfer Layer with Titanium. *Carbon N. Y.* **2023**, *204*, 268–283. [CrossRef]
16. Kim, J.-I.; Lee, W.-Y.; Tokoroyama, T.; Umehara, N. Superlubricity with Graphitization in Ti-Doped DLC/Steel Tribopair: Response on Humidity and Temperature. *ACS Appl. Mater. Interfaces* **2023**, *15*, 19715–19729. [CrossRef]
17. Pauling, L.C. A Resonating-Valence-Bond Theory of Metals and Intermetallic Compounds. *Proc. R. Soc. Lond. Ser. A Math. Phys. Sci.* **1949**, *196*, 343–362. [CrossRef]
18. Cui, X.; Li, P.; Lei, H.; Tu, C.; Wang, D.; Wang, Z.; Chen, W. Greatly Enhanced Tribocatalytic Degradation of Organic Pollutants by TiO_2 Nanoparticles through Efficiently Harvesting Mechanical Energy. *Sep. Purif. Technol.* **2022**, *289*, 120814. [CrossRef]
19. Bunriw, W.; Harnchana, V.; Chanthad, C.; Huynh, V.N. Natural Rubber-TiO_2 Nanocomposite Film for Triboelectric Nanogenerator Application. *Polymers* **2021**, *13*, 2213. [CrossRef]
20. Tokoroyama, T.; Tagami, Y.; Murashima, M.; Lee, W.Y.; Umehara, N.; Kousaka, H. Tribological Property of Ta-CNx:Ta Deposited via Ion Beam Assisted-Filtered Arc Deposition. *Tribol. Int.* **2022**, *168*, 107450. [CrossRef]

21. Parvizian, F.; Ansari, F.; Bandehali, S. Oleic Acid-Functionalized TiO_2 Nanoparticles for Fabrication of PES-Based Nanofiltration Membranes. *Chem. Eng. Res. Des.* **2020**, *156*, 433–441. [CrossRef]
22. Dobrenizki, L.; Tremmel, S.; Wartzack, S.; Hoffmann, D.C.; Brögelmann, T.; Bobzin, K.; Bagcivan, N.; Musayev, Y.; Hosenfeldt, T. Efficiency Improvement in Automobile Bucket Tappet/Camshaft Contacts by DLC Coatings—Influence of Engine Oil, Temperature and Camshaft Speed. *Surf. Coat. Technol.* **2016**, *308*, 360–373. [CrossRef]
23. Challagulla, S.; Tarafder, K.; Ganesan, R.; Roy, S. Structure Sensitive Photocatalytic Reduction of Nitroarenes over TiO_2. *Sci. Rep.* **2017**, *7*, 8783. [CrossRef]
24. Lu, J.; Tsai, C.J. Hydrothermal Phase Transformation of Hematite to Magnetite. *Nanoscale Res. Lett.* **2014**, *9*, 230. [CrossRef]
25. Khaemba, D.N.; Neville, A.; Morina, A. A Methodology for Raman Characterisation of MoDTC Tribofilms and Its Application in Investigating the Influence of Surface Chemistry on Friction Performance of MoDTC Lubricants. *Tribol. Lett.* **2015**, *59*, 38. [CrossRef]
26. Imperial, A.; Pe-Piper, G.; Piper, D.J.W.; Grey, I.E. Identifying Pseudorutile and Kleberite Using Raman Spectroscopy. *Minerals* **2022**, *12*, 1210. [CrossRef]
27. Wang, A.; Kuebler, K.E.; Jolliff, B.L.; Haskin, L.A. Raman Spectroscopy of Fe-Ti-Cr-Oxides, Case Study: Martian Meteorite EETA79001. *Am. Mineral.* **2004**, *89*, 665–680. [CrossRef]
28. Ajito, K.; Nagahara, L.A.; Tryk, D.A.; Hashimoto, K.; Fujishima, A. Study of the Photochromic Properties of Amorphous MoO3 Films Using Raman Microscopy. *J. Phys. Chem.* **1995**, *99*, 16383–16388. [CrossRef]
29. Biesinger, M.C.; Lau, L.W.M.; Gerson, A.R.; Smart, R.S.C. Resolving Surface Chemical States in XPS Analysis of First Row Transition Metals, Oxides and Hydroxides: Sc, Ti, V, Cu and Zn. *Appl. Surf. Sci.* **2010**, *257*, 887–898. [CrossRef]
30. Lindberg, B.J.; Hamrin, K.; Johansson, G.; Gelius, U.; Fahlman, A.; Nordling, C.; Siegbahn, K. Molecular Spectroscopy by Means of Esca. *Phys. Scr.* **1970**, *1*, 286–298. [CrossRef]
31. Benoist, L.; Gonbeau, D.; Pfister-Guillouzo, G.; Schmidt, E.; Meunier, G.; Levasseur, A. X-ray Photoelectron Spectroscopy Characterization of Amorphous Molybdenum Oxysulfide Thin Films. *Thin Solid Films* **1995**, *258*, 110–114. [CrossRef]
32. Licklederer, M.; Cha, G.; Hahn, R.; Schmuki, P. Ordered Nanotubular Titanium Disulfide (TiS_2) Structures: Synthesis and Use as Counter Electrodes in Dye Sensitized Solar Cells (DSSCs). *J. Electrochem. Soc.* **2019**, *166*, H3009–H3013. [CrossRef]
33. Halim, J.; Cook, K.M.; Eklund, P.; Rosen, J.; Barsoum, M.W. XPS of Cold Pressed Multilayered and Freestanding Delaminated 2D Thin Films of Mo_2TiC_2Tz and $Mo_2Ti_2C_3Tz$ (MXenes). *Appl. Surf. Sci.* **2019**, *494*, 1138–1147. [CrossRef]
34. Ignaszak, A.; Song, C.; Zhu, W.; Zhang, J.; Bauer, A.; Baker, R.; Neburchilov, V.; Ye, S.; Campbell, S. Titanium Carbide and Its Core-Shelled Derivative TiC@TiO_2 as Catalyst Supports for Proton Exchange Membrane Fuel Cells. *Electrochim. Acta* **2012**, *69*, 397–405. [CrossRef]
35. Ohara, K.; Hanyuda, K.; Kawamura, Y.; Omura, K.; Kameda, I.; Umehara, N.; Kousaka, H. Analysis of Wear Track on DLC Coatings after Sliding with MoDTC-Containing Lubricants. *Tribol. Online* **2017**, *12*, 110–116. [CrossRef]
36. De Feo, M.; Minfray, C.; De Barros Bouchet, M.I.; Thiebaut, B.; Le Mogne, T.; Vacher, B.; Martin, J.M. Ageing Impact on Tribological Properties of MoDTC-Containing Base Oil. *Tribol. Int.* **2015**, *92*, 126–135. [CrossRef]
37. Onodera, T.; Miura, R.; Suzuki, A.; Tsuboi, H.; Hatakeyama, N.; Endou, A.; Takaba, H.; Kubo, M.; Miyamoto, A. Development of a Quantum Chemical Molecular Dynamics Tribochemical Simulator and Its Application to Tribochemical Reaction Dynamics of Lubricant Additives. *Model. Simul. Mater. Sci. Eng.* **2010**, *18*, 034009. [CrossRef]
38. Deshpande, P.; Minfray, C.; Dassenoy, F.; Thiebaut, B.; Le Mogne, T.; Vacher, B.; Jarnias, F. Tribological Behaviour of TiO_2 Atmospheric Plasma Spray (APS) Coating under Mixed and Boundary Lubrication Conditions in Presence of Oil Containing MoDTC. *Tribol. Int.* **2018**, *118*, 273–286. [CrossRef]
39. Deshpande, P.; Minfray, C.; Dassenoy, F.; Le Mogne, T.; Jose, D.; Cobian, M.; Thiebaut, B. Tribocatalytic Behaviour of a TiO_2 Atmospheric Plasma Spray (APS) Coating in the Presence of the Friction Modifier MoDTC: A Parametric Study. *RSC Adv.* **2018**, *8*, 15056–15068. [CrossRef]
40. Galhenage, R.P.; Yan, H.; Rawal, T.B.; Le, D.; Brandt, A.J.; Maddumapatabandi, T.D.; Nguyen, N.; Rahman, T.S.; Chen, D.A. MoS_2 Nanoclusters Grown on TiO_2: Evidence for New Adsorption Sites at Edges and Sulfur Vacancies. *J. Phys. Chem. C* **2019**, *123*, 7185–7201. [CrossRef]
41. Waqas, M.; Zahid, R.; Bhutta, M.U.; Khan, Z.A.; Saeed, A. A Review of Friction Performance of Lubricants with Nano Additives. *Materials* **2021**, *14*, 6310. [CrossRef]
42. Kim, J.; Lee, W.Y.; Tokoroyama, T.; Murashima, M.; Umehara, N. Friction Characteristics of Amorphous Carbon Coating against Various 3d-Transition Metals. *Tribol. Int.* **2022**, *174*, 107690. [CrossRef]
43. Gao, Y.; Sun, R.; Zhang, Z.; Xue, Q. Tribological Properties of Oleic Acid—Modified TiO_2 Nanoparticle in Water. *Mater. Sci. Eng. A* **2000**, *286*, 149–151. [CrossRef]
44. Gao, Y.; Chen, G.; Oli, Y.; Zhang, Z.; Xue, Q. Study on Tribological Properties of Oleic Acid-Modified TiO_2 Nanoparticle in Water. *Wear* **2002**, *252*, 454–458. [CrossRef]
45. Grossiord, C.; Varlot, K.; Martin, J.M.; Le Mogne, T.; Esnouf, C.; Inoue, K. MoS_2 Single Sheet Lubrication by Molybdenum Dithiocarbamate. *Tribol. Int.* **1998**, *31*, 737–743. [CrossRef]
46. Luttrell, T.; Halpegamage, S.; Tao, J.; Kramer, A.; Sutter, E.; Batzill, M. Why Is Anatase a Better Photocatalyst than Rutile?—Model Studies on Epitaxial TiO_2 Films. *Sci. Rep.* **2015**, *4*, 4043. [CrossRef]

47. Kajdas, C.; Hiratsuka, K. Tribochemistry, Tribocatalysis, and the Negative-Ion-Radical Action Mechanism. *Proc. Inst. Mech. Eng. Part J J. Eng. Tribol.* **2009**, *223*, 827–848. [CrossRef]
48. Hiratsuka, K.; Kajdas, C.; Yoshida, M. Tribo-Catalysis in the Synthesis Reaction of Carbon Dioxide. *Tribol. Trans.* **2004**, *47*, 86–93. [CrossRef]
49. Hiratsuka, K.; Kajdas, C. Mechanochemistry as a Key to Understand the Mechanisms of Boundary Lubrication, Mechanolysis and Gas Evolution during Friction. *Proc. Inst. Mech. Eng. Part J J. Eng. Tribol.* **2013**, *227*, 1191–1203. [CrossRef]
50. Kajdas, C. Importance of Mechanochemistry and Tribochemistry for Tribology. *Tribol. Schmier.* **2013**, *60*, 45–50.
51. Khaemba, D.N.; Neville, A.; Morina, A. New Insights on the Decomposition Mechanism of Molybdenum DialkyldiThioCarbamate (MoDTC): A Raman Spectroscopic Study. *RSC Adv.* **2016**, *6*, 38637–38646. [CrossRef]
52. Koike, R.; Suzuki, A.; Kurihara, K.; Adachi, K. Formation of Low Friction Interface under Sliding Contact between Bearing Steels in MoDTC Oil. *Toraibarojisuto/J. Jpn. Soc. Tribol.* **2019**, *64*, 250–258.
53. Koike, R.; Suzuki, A.; Kurihara, K.; Adachi, K. Formation of Nano Interface by Sliding between Hard Coatings and Metals in MoDTC Contained Oil. *Tribol. Online* **2022**, *17*, 1–8. [CrossRef]
54. Fan, F.R.; Xie, S.; Wang, G.W.; Tian, Z.Q. Tribocatalysis: Challenges and Perspectives. *Sci. China Chem.* **2021**, *64*, 1609–1613. [CrossRef]
55. Shin, E.C.; Ko, J.H.; Lyeo, H.K.; Kim, Y.H. Derivation of a Governing Rule in Triboelectric Charging and Series from Thermoelectricity. *Phys. Rev. Res.* **2022**, *4*, 023131. [CrossRef]

Disclaimer/Publisher's Note: The statements, opinions and data contained in all publications are solely those of the individual author(s) and contributor(s) and not of MDPI and/or the editor(s). MDPI and/or the editor(s) disclaim responsibility for any injury to people or property resulting from any ideas, methods, instructions or products referred to in the content.